Catalysis Today 138 (2008) 187–192

Contents lists available at ScienceDirect

Catalysis Today

journal homepage: www.elsevier.com/locate/cattod

Catalytic monoliths for ethanol steam reforming

Albert Casanovas [a], Carla de Leitenburg [b], Alessandro Trovarelli [b], Jordi Llorca [a,*]

[a] Institut de Tècniques Energètiques, Universitat Politècnica de Catalunya, Av. Diagonal 647, Ed. ETSEIB, 08028 Barcelona, Spain
[b] Dipartimento de Scienze e Tecnologie Chimiche, Università di Udine, via del Cotonificio 108, 33100 Udine, Italy

ARTICLE INFO

Article history:
Available online 16 July 2008

Keywords:
Hydrogen
Monolith
Ethanol steam reforming
Water gas shift
Cobalt

ABSTRACT

Cordierite monoliths coated with Co/ZnO catalysts were prepared by washcoating, urea, and sol–gel techniques and characterized by confocal microscopy, scanning electron microscopy (SEM), transmission electron microscopy, X-ray photoelectron spectroscopy (XPS), temperature-programmed reduction (TPR), and adherence tests. The performance of the catalytic monoliths for practical application in the production of hydrogen through ethanol steam reforming (ESR) and water gas shift (WGS) reactions was evaluated. Monoliths prepared by the urea method exhibited excellent dispersion and adherence of catalyst coatings and performed better for the reforming of ethanol. 5.6 mol H_2/mol C_2H_5OH were obtained from a C_2H_5OH:H_2O = 1:6 gaseous mixture at 723 K and 0.33 mL min^{-1} of C_2H_5OH. Under these conditions and total ethanol conversion the composition of the effluent stream was 73.9% H_2, 23.7% CO_2, 1.2% CO, and 1.0% CH_4. The amount of CO was kept low due to the activity of monoliths for the WGS reaction under ethanol steam reforming conditions.

1. Introduction

Hydrogen production processes are currently being thoroughly investigated owing to the possibility of using hydrogen as an energy carrier in the development of fuel cell technologies. Nowadays, hydrogen is mainly produced by steam reforming of natural gas, a fossil fuel, but in order to develop a more sustainable energy model it is highly desirable to incorporate renewable sources to the generation of hydrogen. One of these sources could be bioethanol, which is a liquid biofuel with high energy density that can be obtained easily in a variety of locations from many biomass sources [1]. In addition, a bioethanol-to-H_2 system has the advantage of being CO_2 neutral. There are numerous studies that demonstrate the feasibility of generating hydrogen from ethanol–water mixtures through catalytic steam reforming [2,3]: $CH_3CH_2OH + 3H_2O \rightarrow 6H_2 + 2CO_2$. Among all catalysts tested so far, those based on ZnO-supported cobalt exhibit the highest activity and selectivity towards hydrogen at low temperature [4–6]. The yield of hydrogen obtained with a conventional Co/ZnO catalyst (10% Co, w/w) prepared by impregnation is about 5.5 mol of H_2/mol of ethanol at 623 K. In addition, the stability of these catalysts can be further improved by the addition of promoters, such as Na^+ [7]. However, all these studies have been carried out over ZnO-supported cobalt catalysts in powder form, which are not useful for industrial environments or for mobile applications, such as fuel cell powered vehicles equipped with internal reformers. Conversely, in these applications monolithic structures can be used as a support to obtain catalytic reactors with good structural and thermal stability, minimize pressure drop and avoid reactor blocking [8,9]. Recently, it has been shown that conventional ceramic monoliths can be used as appropriate structured supports for Ni/La_2O_3 and Ru/γ-Al_2O_3 catalysts in oxidative reforming of ethanol [10,11]. These studies have focused on catalytic performance and no data concerning catalyst dispersion, adherence, and stability has been reported. In this work we have prepared a series of ceramic monoliths coated with Co/ZnO catalysts with high thermal and mechanical stability for the generation of hydrogen by steam reforming of ethanol in practical devices. Monoliths have been prepared by washcoating, urea, and sol–gel methods, studied in detail by several characterization techniques, and tested under ethanol steam reforming (ESR) and water gas shift (WGS) conditions.

2. Experimental

2.1. Preparation of monoliths

400 cells per square inch (cpsi) cordierite monolith cylinders with a diameter of 2 cm and a length of 2 cm were used. They were obtained by cutting larger monolith pieces with a diamond saw. Monoliths were coated with Co/ZnO by three different methods: ex situ washcoating, in situ urea precipitation, and in situ sol–gel

* Corresponding author. Tel.: +34 93 401 17 08; fax: +34 93 401 71 49.
E-mail address: jordi.llorca@upc.edu (J. Llorca).

0920-5861/$ – see front matter © 2008 Elsevier B.V. All rights reserved.
doi:10.1016/j.cattod.2008.05.028

method. In the first method (washcoating method), a Co/ZnO (10% Co, w/w) powder catalyst was first prepared by incipient wetness impregnation using an aqueous solution of cobalt nitrate as precursor. The solid was dried at 373 K overnight and calcined in air at 673 K for 6 h. Monoliths were dipped in a dense, vigorously agitated suspension (~5%, w/w) of Co/ZnO in de-ionized water. After each immersion monoliths were dried at 373 K with continuous rotation and then calcined at 673 K. This procedure was repeated several times in order to obtain the desired weight gain (14–17%, w/w). Monoliths were prepared by the washcoating method with and without the presence of SiO_2 as a binder (SiO_2:catalyst = 1:19 on a weight basis). These monoliths were labeled as WS-CoZn and W-CoZn, respectively. The second method used for the functionalization of monoliths consisted in the co-precipitation of Co^{2+} and Zn^{2+} precursors inside the channels of the monoliths by the effect of pH increase by urea decomposition. Monoliths were dipped in a solution that contained the nitrate metal salts and the precipitating agent (Co:ZnO = 1:10 weight basis, M^{2+}:urea = 1:1 molar basis). After filling the channels completely with the solution, monoliths were heated at 343 K under continuous rotation for 12 h in order to decompose urea and increase the pH smoothly ($CO(NH_2)_2 + 3H_2O \rightarrow CO_2 + 2NH_4^+ + 2OH^-$), which resulted in the co-precipitation of cobalt and zinc salts. After that, monoliths were dried at 383 K and calcined at 673 K. These monoliths were labeled as U-CoZn and ca. 18% of weight gain was attained. The third method for coating cordierite monoliths with Co/ZnO consisted in a sol–gel method [12]. Monoliths were immersed in a 2-methoxyethanol solution of acetate precursors (0.75 M) and 2-aminoethanol ([M^{2+}]:[2-aminoethanol] = 1:1 on a molar basis) and heated at 333 K for 30 min, then dried at 383 K and calcined at 823 K for 2 h. This procedure was repeated several times in order to obtain a weight gain similar to previous methods.

2.2. Characterization

Three-dimensional, non-invasive assessment of the microgeometry of the interior of monolith channels was performed by confocal microscopy with a SENSOFAR PLμ 2300 optical imaging profiler. The walls of the channels were scanned at a step height of 4 μm, and the total height analyzed was about 300 μm. Surface roughness is given by the average roughness value, R_a, which is the arithmetic mean of the departure of the profile from the center line of a line scan of the surface. Mechanical stability was evaluated by two different methods. In one method, the monoliths were immersed in water and exposed to high frequency ultrasounds (40 KHz). Weight loss was monitored for 30 min. In the second method, monoliths were exposed directly to mechanical vibration. The vibration frequency was raised progressively from 20 to 50 Hz at a fixed acceleration value of 2 G, and from 50 to 100 Hz at acceleration values between 5 and 15 G. Weight loss was monitored after 30 min at each frequency, and after 3 h under the most severe vibration conditions (100 Hz, 15 G). G levels were controlled directly on the vibration test board with a Brüel & Kjaer 4370 accelerometer. The microstructure, morphology, and composition of monolith channels were studied by scanning electron microscopy (SEM) and energy dispersive X-ray analysis (EDX). Secondary and backscattered electron images were recorded at 20 kV using a JEOL JSM 6400 microscope. High-resolution transmission electron microscopy (HRTEM) was conducted at 200 kV with a JEOL JEM 2010F microscope equipped with a field emission gun. Samples were dispersed in alcohol and deposited on grids with holey carbon films. For surface analysis, X-ray photoelectron spectroscopy (XPS) was performed with a PerkinElmer PHI-5500 instrument equipped with an Al X-ray source operated at 12.4 kV and a hemispherical electron analyzer. For each monolith analyzed, spectra were recorded over the catalyst coating at different locations by using a broad incident beam of about 0.5 mm of diameter. Surface area measurements (BET) were performed with a Micromeritics TriStar 3000 apparatus. Temperature programmed reduction (TPR) was carried out with a Micromeritics AutoChem II 2920 instrument using a H_2/Ar mixture (5% H_2) at 10 K min^{-1} and a TCD detector.

2.3. Catalytic tests

Ethanol steam reforming was carried out at atmospheric pressure in a stainless steel tubular reactor at a total flow of 80 mL min^{-1}. C_2H_5OH (0.33 mL min^{-1}) and H_2O were fed separately at a C_2H_5OH:H_2O molar ratio of 1:6 and the mixture was balanced with He. The effluent of the reactor was monitored on line with a MKS Cirrus mass spectrometer. H_2, CO, CO_2, CH_4, CH_3CHO, CH_3COCH_3, CH_3COOH, H_2O, and C_2H_5OH partial pressures were calibrated using appropriate standards and an Agilent micro-GC. In a typical experiment, the monolith was first pretreated inside the reactor with a H_2:N_2 mixture (50 mL min^{-1}, 1, 10% H_2) at 723 K for 4 h, and the reaction mixture introduced at 473 K. The reaction was followed for one temperature cycle 473–773–473 K (2 K min^{-1}). Monoliths operated under isothermal conditions as deduced from temperature monitoring inside their channels, located either in contact with the reactor wall or at the center of the reactor. The water gas shift reaction was carried out at atmospheric pressure in the 473–673 K temperature range using a CO:H_2:H_2O:N_2 = 1:2:6:14 molar mixture (total flow 50 mL min^{-1}). Water was provided with a syringe pump and vaporized before entering the reactant stream. Analysis of products was performed with a Varian micro-GC.

3. Results and discussion

3.1. Stability of catalyst coatings

Mechanical stability of the catalytically active phase in monoliths is a critical issue for practical application purposes because coating loss and banking up should be completely avoided. In this regard, the characteristics of monoliths prepared by co-precipitation using urea as a precipitating agent (U-CoZn) and by sol–gel (G-CoZn) were considerably different from those prepared by traditional washcoating techniques (W-CoZn and WS-CoZn). Fig. 1 shows the weight loss of monoliths under standard ultrasound testing conditions. The graph shows that the adherence of coatings in monoliths U-CoZn and G-CoZn were unexpectedly high. After 30 min of ultrasound exposure, less than 4% of the

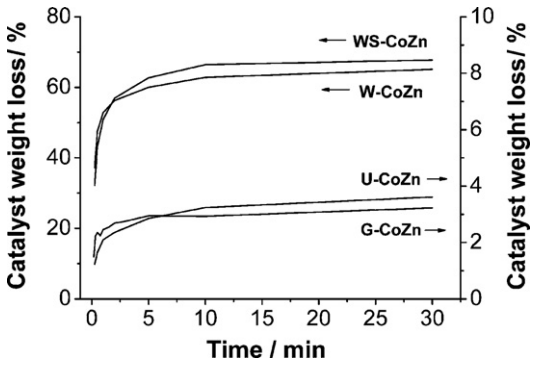

Fig. 1. Plot of monolith weight loss over time caused by ultrasound exposure of monoliths immersed in water.

catalytically active phase was lost. In contrast, Co/ZnO monoliths prepared by washcoating methods (W-CoZn and WS-CoZn) exhibited rather poor coating adherence, and more than 50% of the catalyst loading was lost after only 1 min of ultrasound exposure. Also, the binding effect of silica was hardly recognizable. Exposure of monoliths U-CoZn and G-CoZn directly to mechanical vibration up to 100 Hz and 15 G resulted in negligible catalyst loss (less than 1%). The excellent performance of monoliths U-CoZn and G-CoZn during mechanical stability tests is ascribed to the presence of intermediate complexes [13] during thermal decomposition of precursors, which may act as strong linking agents with cordierite. We have also studied the stability of catalytic monoliths after steam treatments in order to simulate aging conditions. Thermal stability tests were designed for simulating continuous switch on and shut down of a reformer unit by oscillating the temperature between 333 and 723 K (5 K min^{-1}) under a continuous H_2O/N_2 flow (6 mL min^{-1} H_2O, 25 mL min^{-1} total). No differences in adherence of catalyst coatings were observed after four consecutive cycles.

3.2. SEM–EDX

Cross-section analysis of washcoated monoliths by scanning electron microscopy revealed the characteristic morphology expected for this type of preparation method [8,9], with catalyst particles preferably deposited at the channel corners. The coating thickness typically varied between 20 and 200 μm and no significant differences existed between samples prepared by washcoating with SiO_2. In contrast, the structure of monoliths U-CoZn and G-CoZn was much more uniform and no apparent accumulation of catalyst particles was observed at the corners, being the coating thickness less than ca. 20 μm all around the channels. The microstructure and composition of the catalytically active phase in each monolith was also studied in detail by SEM–EDX inside the channels (Fig. 2). Scanning electron microscopy images of catalyst particles deposited by the washcoating method (Fig. 2a) showed aggregates with no particular morphology at the micrometer-size level, typical of supported catalysts. Semi-quantitative energy dispersive X-ray analysis performed over the catalyst particles showed, in all cases, Zn to Co atomic ratios close to the bulk composition of Co/Zn∼0.1. In contrast, the microstructures of catalyst layers in monoliths U-CoZn (Fig. 2b) and G-CoZn (Fig. 2c) were quite distinctive. In both cases the coating was constituted by a fine-grained, homogeneous groundmass and, in the case of U-CoZn, also by discrete, euhedral ZnO crystallites of about 1 μm in size. The excellent homogeneity of catalyst coatings in these monoliths is well exemplified by the fact that cordierite macropores were covered and preserved after catalyst coating. The BET surface area measured directly on U-CoZn and G-CoZn was 1.1 and 1.7 $m^2 g^{-1}$, respectively (the BET of the cordierite monolith was 0.1 $m^2 g^{-1}$). The different coating adherence exhibited by monoliths U-CoZn and G-CoZn with respect to that of W-CoZn and WS-CoZn described in the precedent section are well explained considering the structure and morphology of the respective catalyst layers. All preparation methods lead to the formation of fine catalyst particles, but monoliths U-CoZn and G-CoZn show a more compact coating structure which results in much better adherence. The distribution and morphology of catalyst coatings was maintained after steam aging.

3.3. Confocal microscopy

Fig. 3 shows three-dimensional roughness maps corresponding to the interior of representative channels of a U-CoZn monolith before and after preparation. As expected, the interior of a cordierite channel is flat, and the roughness (R_a = 3.3) comes basically from the procedure used for monolith fabrication. Large pores are distributed randomly all over the channel walls, which are visible as black areas in Fig. 3a. The confocal profile image of monolith U-CoZn is shown in Fig. 3b. It is evident that the distribution of the catalytically active phase is extremely homogeneous along the channel and that a moderate curvature takes place at the corners, in accordance to SEM results. The profile analysis revealed that the maximum difference in coating thickness across the channels was less than 10 μm, and that the surface roughness was close to that of naked monoliths. This is an additional proof that the coating was homogeneously expanded over the channel interior. In contrast to this, the distribution of catalyst particles inside the channels of monoliths W-CoZn and WS-CoZn was more heterogeneous and less reproducible, with surface roughness values up to R_a = 9.8, according to a disordered deposition of catalyst particles.

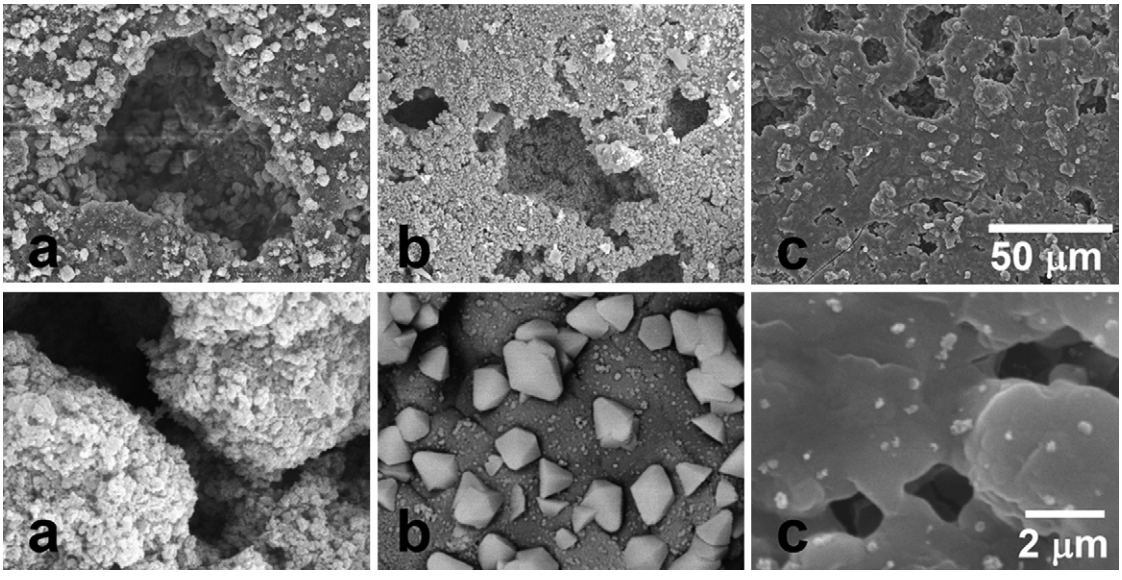

Fig. 2. Scanning electron microscopy images of monoliths W-CoZn (a), U-CoZn (b), and G-CoZn (c) at different magnification.

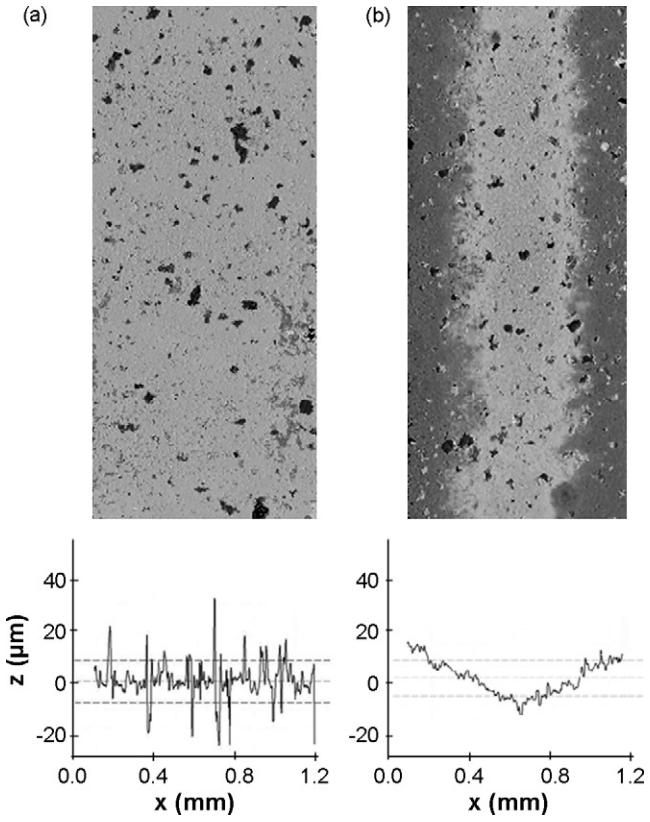

Fig. 3. Three-dimensional confocal images and transversal profile sections corresponding to the interior of naked monolith channels (a) and U-CoZn (b).

3.4. XPS

Several X-ray photoelectron spectra were recorded over monoliths U-CoZn and G-CoZn in order to obtain Co/Zn ratios at the surface and to check for chemical homogeneity of catalyst coatings within the same monolith. Atomic Co/Zn ratios recorded over different areas of monoliths U-CoZn and W-CoZn were in the range 0.16–0.24 and 0.30–0.34, respectively, whereas the values obtained over monolith G-CoZn were in the range 0.81–0.92. Therefore, reasonably similar Co/Zn values were found within the same monolith, suggesting homogeneous coating composition. Concerning the chemical state of Co and Zn, binding energy values corresponded to the respective oxides, as expected.

3.5. HRTEM

A detailed transmission electron microscopy study was performed over the catalyst coating of monolith U-CoZn after exposure to hydrogen at 723 K because its preparation method turned to be the best in terms of adherence, homogeneity, reproducibility, and simplicity. Fig. 4 shows images recorded at different magnification. In the low-magnification image (Fig. 4a), spherical cobalt particles of about 10–30 nm in diameter are well mixed with ZnO. Under high-resolution conditions (Fig. 4b), cobalt particles exhibit a core-shell structure, with Co metal cores (lattice spacing at 2.0 Å of fcc (1 1 1) or hcp (0 0 2) in the FT image) covered by a thick layer (around 5 nm) of cobalt oxide (lattice spacings at 2.3–2.4 Å). The core-shell structure and size of cobalt particles in U-CoZn is fairly similar to that reported for the Co/ZnO catalyst powder used here for preparing monolith W-CoZn [5]. However, the contact area between cobalt particles and ZnO is much larger in U-CoZn, suggesting a stronger interaction of Co particles with the support. The contact angle has increased from $<60^\circ$ for the impregnated sample to $>90^\circ$ in U-CoZn.

3.6. Ethanol steam reforming

Monolith U-CoZn was tested in the ESR reaction without any pretreatment and after exposure to hydrogen at 723 K. Fig. 5 shows the reactor effluent in both cases in terms of partial pressures of reactants (C_2H_5OH and H_2O), products (H_2, CO and CO_2), and side products (CH_4, acetaldehyde, and dimethylketone) during a 473–773–473 temperature cycle. In the absence of pretreatment (Fig. 5a) the main products of the reaction were hydrogen and acetaldehyde, indicating that the main reaction was the dehydrogenation of ethanol ($C_2H_5OH \rightarrow CH_3CHO + H_2$). Minor amounts of CO_2 and dimethylketone were also obtained as a result of acetaldehyde condensation ($2CH_3CHO + H_2O \rightarrow (CH_3)_2CO + CO_2 + 2H_2$). Therefore, no true reforming of ethanol took place on the monolith as prepared and, consequently, the hydrogen production was rather low. In contrast, the catalytic performance changed drastically when the monolith was exposed to hydrogen at 723 K prior to reaction (Fig. 5b). In this case, high amounts of H_2 and CO_2 were obtained at 723–773 K and, simultaneously, the mass signal corresponding to water decreased, thus indicating that reforming of ethanol was

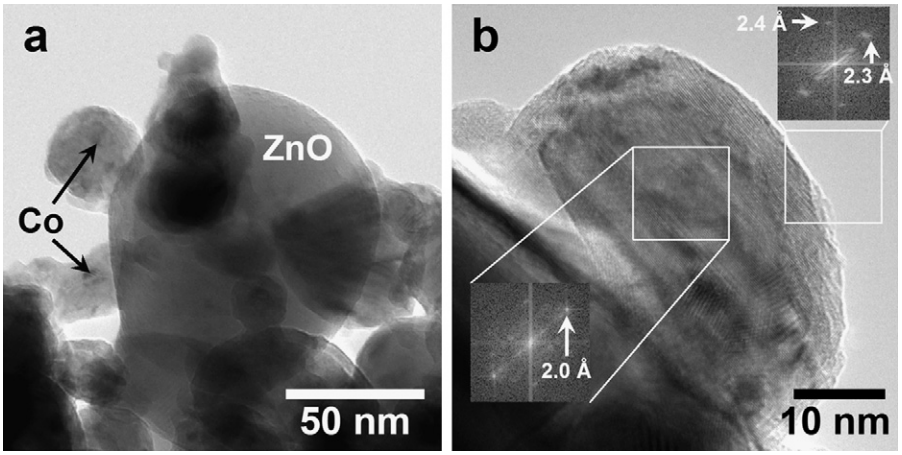

Fig. 4. Bright field (a) and high resolution (b) transmission electron microscopy images of catalyst particles inside monolith U-CoZn. Fourier transform images of selected areas are also included.

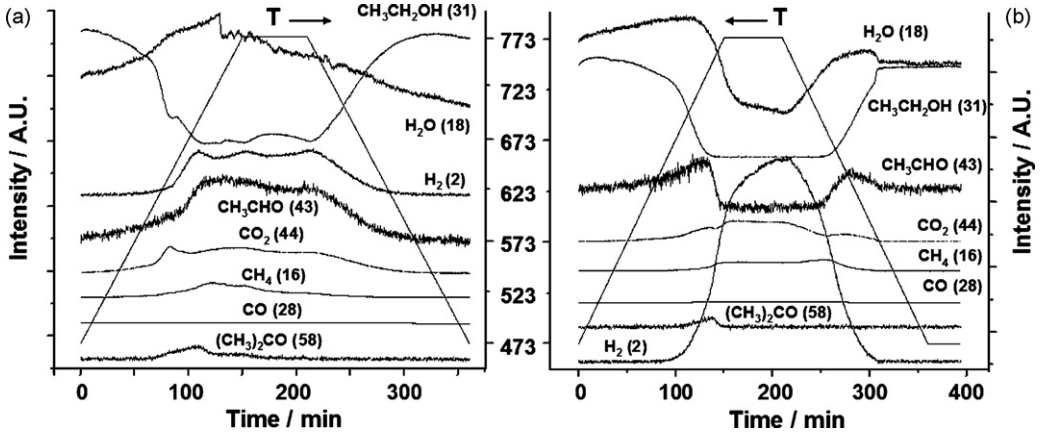

Fig. 5. Product distribution in the ethanol steam reforming reaction over monolith U-CoZn before (a) and after (b) treatment with H_2 at 723 K. $C_2H_5OH:H_2O = 1:6$, 0.33 mL min^{-1} C_2H_5OH, total flow 80 mL min^{-1}.

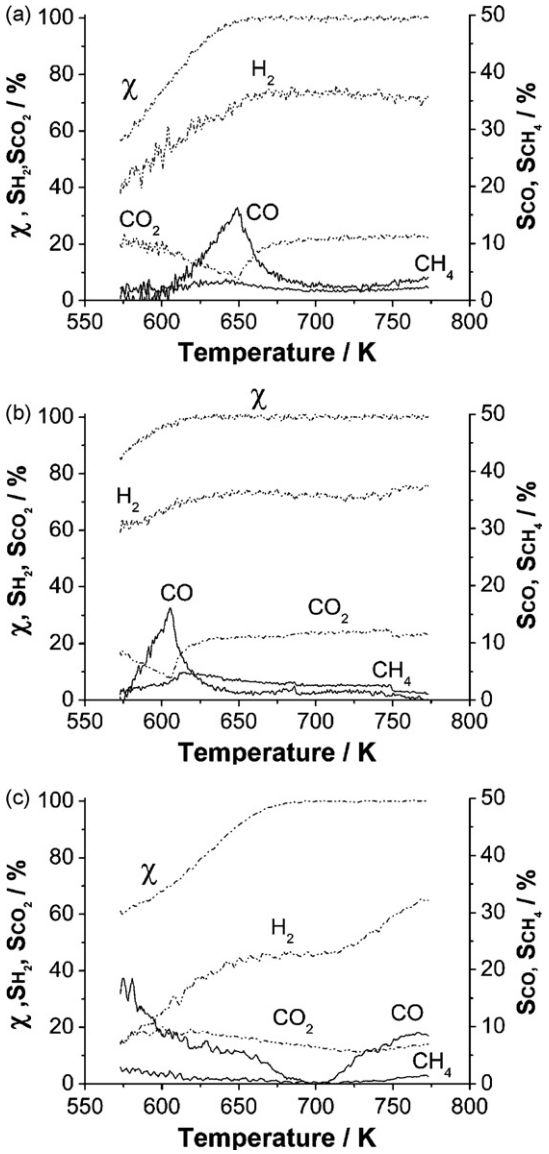

Fig. 6. Performance of monoliths W-CoZn (a), U-CoZn (b), and G-CoZn (c) in the steam reforming of ethanol at different temperature. Selectivity values are reported on a dry basis. $C_2H_5OH:H_2O = 1:6$, 0.33 mL min^{-1} C_2H_5OH, total flow 80 mL min^{-1}.

operative ($C_2H_5OH + 3H_2O \rightarrow 6H_2 + 2CO_2$). In addition to minor amounts of CH_4, acetaldehyde and dimethylketone were also observed as intermediate species at a lower temperature. These results are in accordance with a reaction scheme where ethanol dehydrogenates first to acetaldehyde at low temperature and then steam reforming proceeds over metallic Co [14]. The generation of metallic Co upon the reduction pretreatment with hydrogen may be favored by both the core-shell Co/Co_3O_4 nanoparticle structure and strong interaction with ZnO. Temperature programmed reduction of monolith U-CoZn contained two hydrogen consumption signals at about 573 and 698 K, which are ascribed to the two-step reduction of Co_3O_4 into metallic Co via the formation of CoO [15]. Similar TPR profiles were recorded for monoliths G-CoZn and W-CoZn.

The behavior of the different monoliths for ESR after activation is shown in Fig. 6. At low temperatures (<673 K) ethanol conversion was considerably higher for monolith U-CoZn with respect to W-CoZn and G-CoZn. Monoliths U-CoZn and W-CoZn showed good selectivity towards H_2 under total ethanol conversion (>648–673 K). Also, for U-CoZn and W-CoZn, selectivity values of H_2 and CO_2 were nearly stoichiometric, 73 and 23%, respectively. In contrast, monolith G-CoZn required higher temperature for performing ESR (>723 K), but this was accompanied by an increase in CO production and, consequently, in lower hydrogen yield. Therefore, the performance of monoliths for ESR can be ordered as follows: U-CoZn > W-CoZn ≫ G-CoZn.

3.7. Water gas shift

The amount of CO obtained in the ESR experiments was well below the equilibrium value, suggesting that monoliths were

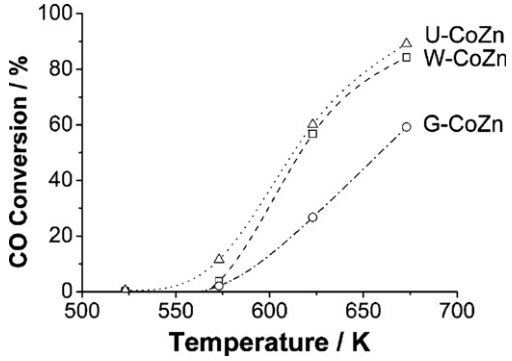

Fig. 7. Activity of monoliths in terms of CO conversion in the water gas shift reaction. $CO:H_2:H_2O:N_2 = 1:2:6:14$, total flow 50 mL min^{-1}.

active for the WGS reaction under ethanol steam reforming conditions. Fig. 7 shows the conversion of CO attained with the different monoliths under conditions simulating the outlet of an ethanol steam reformer ($CO:H_2:H_2O = 1:2:6$). In all cases conversion of CO increased with temperature, particularly in the 573–673 K temperature range, strongly suggesting that the low amount of CO obtained under ESR conditions was partly due to WGS activity of catalytic monoliths. Among them, monolith U-CoZn was the most active for WGS and, consequently, this sample yielded less CO during ethanol steam reforming. In addition, monolith G-CoZn, which showed the largest amount of CO during ESR, showed the lowest activity towards WGS, too.

4. Conclusions

The preparation route of catalytic monoliths where the active phase is a mixture of cobalt and zinc oxides has a strong influence on both the homogeneity and stability of the catalyst coatings as well as on the performance for the steam reforming of ethanol for producing hydrogen. Conventional preparation by washcoating methods results in catalytic coatings with poor adherence and homogeneity, whereas monoliths prepared by in situ co-precipitation with urea and sol–gel methods exhibit excellent adherence and stability, even after thermal aging with steam. Catalytic monoliths prepared by co-precipitation with urea are more active at low temperature and perform better in the ethanol steam reforming and water gas shift reactions. The remarkable high selectivity towards the reforming products at 648–773 K, 5.66 mol H_2 and 1.84 mol CO_2 per mol of ethanol in the reactant feed, and the mechanical stability of these monoliths makes them suitable for practical application.

Acknowledgements

We are grateful to Corning for providing us with ceramic monolith samples and to Professors Ferran Laguarta (EUOOT-UPC) and Salvador Cardona (ETSEIB-UPC) for extending the use of confocal profiling and mechanical vibration instruments to us. This work was supported by MEC (ENE2006-06925).

References

[1] F. Frusteri, S. Freni, J. Power Sources 173 (2007) 200.
[2] A. Haryanto, S. Fernando, N. Murali, S. Adhikari, Energy Fuels 19 (2005) 2098.
[3] P.D. Vaidya, A.E. Rodrigues, Chem. Eng. J. 117 (2006) 39.
[4] J. Llorca, N. Homs, J. Sales, P. Ramírez de la Piscina, J. Catal. 209 (2002) 306.
[5] J. Llorca, P. Ramírez de la Piscina, J.A. Dalmon, J. Sales, N. Homs, Appl. Catal. B 43 (2003) 355.
[6] J.A. Torres, J. Llorca, A. Casanovas, M. Domínguez, J. Salvadó, D. Montané, J. Power Sources 169 (2007) 158.
[7] J. Llorca, N. Homs, J. Sales, J.L.G. Fierro, P. Ramírez de la Piscina, J. Catal. 323 (2004) 470.
[8] T.A. Nijhuis, A.E.W. Beers, T. Vergunst, I. Hoek, F. Kapteijn, J.A. Moulijn, Catal. Rev. 43 (2001) 380.
[9] R.M. Heck, S. Gulati, R.J. Farrauto, Chem. Eng. J. 82 (2001) 149.
[10] D.K. Liguras, K. Goundani, X.E. Verikyos, J. Power Sources 130 (2004) 30.
[11] D.K. Liguras, K. Goundani, X.E. Verikyos, Int. J. Hydrogen Energy 29 (2004) 419.
[12] N. Viart, M. Richard-Plouet, D. Muller, G. Pourroy, Thin Solid Films 437 (2003) 1.
[13] O. Carp, L. Patron, A. Reller, J. Thermal Anal. Calorim. 73 (2003) 867.
[14] J. Llorca, P. Ramírez de la Piscina, J.A. Dalmon, N. Homs, Chem. Mater. 16 (2004) 3573.
[15] D. Potoczna-Petru, L. Kepinski, Catal. Lett. 73 (2001) 41.